Journal of Statistical Physics, Vol. 52, Nos. 5/6, 1988

Dynamic and Thermodynamic Consequences of Adsorbate Lateral Interactions in Surface Reaction Kinetics*

M. Silverberg[1,2] **and A. Ben-Shaul**[1]

Received April 4, 1988

The effects of lateral interactions on the two-dimensional distribution of adspecies on solid surfaces and their consequences for reaction kinetics are demonstrated for the bimolecular reactive system $A + B \rightarrow AB$. The discussion concentrates on systems where one reactant, A, is stationary while the other, B, is freely diffusing and instantaneously relaxing. A modified Bethe–Peierls-type lattice gas approximation is formulated in order to account for the rapidly equilibrating distribution of B atoms. The approximation takes into account all nearest and next nearest neighbor interactions between the adspecies and the nonuniformity of the lattice available to B implied by the presence of immobile A's on the surface. This model is combined with a Monte Carlo simulation of the reactive events in order to calculate reaction rates, e.g., in temperature-programmed processes. The rates are compared with full Monte Carlo simulations (for all kinetic processes), showing good agreement between the two schemes, except at very high coverages, where very long range correlations in the system which are ignored in the lattice gas approximation must be taken into account.

KEY WORDS: Surface reactions; adsorbate lateral interactions; islanding; lattice gas approximations; Monte Carlo; temperature-programmed reaction spectroscopy.

1. INTRODUCTION

The rates of kinetic processes taking place on solid surfaces depend crucially on the two-dimensional (2D) distribution of the adspecies and on

---

* This paper is dedicated to Howard Reiss in celebration of his 66th birthday.

[1] Department of Physical Chemistry and Fritz Haber Research Center for Molecular Dynamics, Hebrew University, Jerusalem 91904, Israel.

[2] Present address: Department of Chemistry, Northwestern University, Evanston, Illinois 60208.

0022-4715/88/0900-1179$06.00/0

lateral interactions between the adsorbed particles. Consider, for example, the bimolecular reaction

$$A(s) + B(s) \rightarrow AB(g) \tag{1}$$

in which both reactants are adsorbed on the surface ($s =$ surface), while AB is a rapidly desorbing product ($g =$ gas); the catalytic oxidation of carbon monoxide, $O + CO \rightarrow CO_2$ on, say, platinum surfaes is one of the best known examples for such a process.$^{(1)}$ If A and B are randomly distributed over the surface, then the rate of (1) will be proportional to the product of their coverages, i.e., $R \sim \theta_A \theta_B$, with θ_A denoting the fraction of lattice sites occupied by A, etc. This, however, is a very special case corresponding to a system in which the adspecies do not interact with each other and furthermore their diffusion rates are large compared to the rate of reactive events, so as to ensure instantaneous equilibration at all times. In most systems of interest lateral interactions cannot be ignored (especially at high coverages) and mobilities of different adspecies are often markedly different; e.g., in the $O + CO \rightarrow CO_2$ system the O atoms are essentially stationary while the CO molecules diffuse freely on the surface, at most reaction temperatures.

The effects of lateral interactions on reaction rates are manifested in two (related) aspects: topologically and energetically. By topological effects we refer to the fact that lateral interactions can induce highly nonrandom distributions of the adspecies on the 2D lattice, thereby influencing, e.g., in reaction (1), the frequency of $A + B$ encounters (i.e., occupation of neighboring sites). The energetic effects correspond to the influence of neighboring adspecies on the reaction probability of a potentially reactive A–B pair (i.e., A–B occupying neighboring adsorption sites). This is mainly reflected in the activation barrier for reaction, which may be appreciably modified by lateral interactions between A–B and its local environment.

In order to be a little more specific, let us consider a bimolecular reactive system of the type (1) in which one of the adsorbed reactants (A) is stationary, while the other (B) diffuses rapidly over the remaining ("A-free") lattice sites. We also assume that reaction can only occur when B reaches a lattice site which is a (nearest or other "low-order") neighbor of an A-occupied site. To simplify matters even further, suppose also that the characteristic time of reaction τ_R (i.e., the reciprocal reaction probability of a potentially reactive A–B pair) is considerably longer than τ_B, the time between consecutive random walks of B on the lattice. This last assumption ensures that $\{B|A\}$, the distribution of B atoms on the sublattice of A-free sites, is always in thermodyamic equilibrium.

In a system with nonzero lateral interactions, calculating the 2D distribution of adspecies is nontrivial even for a simple uniform lattice, where all sites are equivalent. This is all the more so for $\{B|A\}$ on the nonuniform sublattice prescribed to B by the quenched distribution of A's ($\{A\}$) in a system with arbitrary B–B and A–B potentials. In our problem we need $\{B|A\}$ to calculate the number of A–B pairs (and their local environments), which determine the rate of reaction R. The calculation of R for a given $\{B|A\}$, and the modification of $\{A\}$ following the removal A–B pairs from the surface, may be simply and efficiently modelled by a Monte Carlo (MC) simulation algorithm, as will be described in Section 2.3. Simulation methods can also be applied to calculate $\{B|A\}$, but are very costly (in terms of computer time) for modeling reactive systems. This is particularly so for systems with varying temperature conditions, as in temperature-programmed reaction experiments which serve as a principal source for kinetic information.

If $\{B|A\}$ is an equilibrium distribution, as we assume here, one might expect that it may be calculated using more "analytical" (and "less expensive") methods than computer simulations. Indeed, we have recently shown how two familiar lattice gas approximations may be reformulated in order to calculate $\{B|A\}$ for an arbitrary given $\{A\}$ in systems governed by nearest neighbor A–B and B–B potentials.(2) These were modified versions of the mean-field (Bragg–Williams), and the quasichemical (Bethe–Guggenheim) approximations (MFA and QCA, respectively). The approximate $\{B|A\}$'s are derived by first expressing the many-particle distribution as a product of singlet (MFA) or doublet (QCA) distributions, which are subsequently determined by minimizing the system free energy subject to conservation (self-consistency) conditions.(2)

The modified lattice gas models for $\{B|A\}$ mentioned above have been incorporated into a more general theoretical modeling scheme for reactive surface processes of the type (1). In this approach MC methods are used to describe the slow temporal evolution of the nonequilibrium $\{A\}$ (i.e., prior to B adsorption) and the $A+B$ reaction-desorption, while the lattice gas models are used to calculate the rapidly relaxing $\{B|A\}$. Comparisons with full MC calculations, i.e., those in which MC methods are used for B diffusion as well, show very good agreement between the two schemes. However, for simplicity, the range of lateral A–A, B–B, and A–B interactions has been limited in these analyses to nearest neighbors only.(2) In most systems of interest lateral interactions extend to next nearest, and quite often to third or even higher order, neighbors. The physical implications are most significant. In particular, the preferred adlayer periodicities will generally be higher than the 1×1 structure characterizing a system with nearest neighbor attractions. This implies the existence of ground-state degeneracy, domain boundary effects, and phase transitions between several ordered states which may be induced by changes in coverage or temperature. Correspondingly, a reasonable lattice gas model for $\{B|A\}$ in such systems should take into account higher order correlations between the adspecies. Such a model, which is an extension of the Bethe–Peierls approximation,(4,5) appropriately modified to account for the existence of quenched $\{A\}$ (or more generally, a nonuniform lattice), is described in Section 2 and compared with MC simulations in Section 3. But before turning to the more technical details, a few remarks should be made regarding the physical significance and the calculation of $\{A\}$, the distribution of the less mobile species.

Lateral interactions between chemisorbed species are typically much smaller than the adsorbate–substrate bond (~ 0.1 eV versus a few eV).(6) Nevertheless, these interactions may be strong enough to favor an ordered phase as the stable thermodynamic state, even at low coverages.(7–9) Thus, if, for instance, the A atoms in (1) strongly attract each other, then an initially disordered distribution (reflecting, e.g., a random adsorption mechanism) will gradually evolve into an ordered phase. An intermediate, nonequilibrium, yet long-lived state which often occurs in the course of a disorder → order transition is characterized by the organization of the A atoms in islands.(7–9) These are finite ordered domains whose further growth slows down considerably due to severe kinetic limitations. Now, suppose that B atoms are added at this stage to the regions between A islands and reaction occurs upon their diffusion and arrival at A-island boundaries. Clearly, in this case R will be very different from the case of random $\{A, B\}$. In fact, if the A islands have smooth boundaries and $\{B|A\}$ is random, one expects(2,7) $R \sim \theta_A^{1/2}[\theta_B/(1-\theta_A)]$. This, however, is a highly idealized special case. Computer simulations reveal quite clearly that the islands formed in the course of a phase transition are typically characterized by polydisperse size distributions and highly ramified "coastlines."(7,8) (Available electron(10) and atom(11) diffraction experiments reveal information about the size of islands but not on their detailed shape. Also, island formation is clearly indicated by many kinetic studies.(12,13)) Such complex island patterns characterize the quenched $\{A\}$ distributions considered here. The islands depicted in Section 3 have been calculated by MC simulations, starting with random $\{A\}$ and letting it evolve according to conserved (Kawaski) MC dynamics, as is frequently done in kinetic analyses of phase transitions.(8,9)

The issues considered in this paper interweave chemical (reaction) and physical (diffusion and phase transition) kinetics with equilibrium statistical thermodynamic considerations. Many physical and chemical problems combining these aspects have previously been studied by Prof. Howard Reiss to whom this volume is dedicated. His well-known contributions to the theory of nucleation (see, e.g., ref. 14) and phase transition kinetics, including its recent implementation in the context of gas-phase chain polymerization (see, e.g., ref. 15), constitute one relevant example. Another work of Reiss which is of direct relevance to the present study is his proof that superposition approximations of all orders can be derived from a variation principle. Our derivations of the modified MFA and QCA mentioned above$^{(7)}$ follow very similar lines.

2. MODEL

2.1. The Constrained Distribution $\{B|A\}$

In the Bethe–Peierls approximation (BPA) for a single adsorbate on a regular two-dimensional (2D) lattice, attention is focused on some arbitrary cluster (colony) of sites on the lattice.$^{(4,5)}$ (Since the lattice is uniform, all clusters of the same size and shape are equivalent.) The size and shape chosen for the colony reflect the range of adsorbate lateral interactions and dictate the accuracy of the model. The basic idea of the method is to treat the colony of sites as a (very small) open system in equilibrium with its surroundings. Correspondingly, a grand partition function is written for all possible states of the colony as specified by the configurations of occupied sites and the corresponding lateral interaction energies. Mean field parameters (Lagrange multipliers) are introduced to account for the interaction of the cluster with its surroundings. These and the chemical potential of the particles are determined by conservation and self-consistency requirements. Models based on these notions have been formulated and applied by Adams$^{(5)}$ in order to calculate unimolecular and bimolecular (associative) desorption spectra in a system containing a single adsorbate interacting via nearest neighbor potentials. Five-site and eight-site clusters are required to account for the unimolecular and bimolecular desorption processes for an ordinary square lattice. (Subject to the limitation of nearest neighbor interactions, the ordinary BPA is essentially equivalent to the QCA.)

Our objective in this section is to describe the generalization of the BPA to systems containing more than one type of adspecies and governed by lateral interactions which extend beyond nearest neighbors. More importantly, recall that we seek $\{B|A\}$, the distribution of B's on the sites not occupied by the immobile A's. Since $\{A\}$ is arbitrary, not all site colonies (of equal size and shape) are equivalent, and the BPA should be modified in order to account for this complication. To be more specific, in describing the appropriate model we consider flat surfaces whose adsorption sites form a regular 2D square lattice, each of which can accommodate only one atom, A or B. For simplicity, we restrict the range of B–B and A–B interactions to nearest and next nearest neighbors. The interaction potentials will be denoted as $w_{IJ,\alpha}$ with I, $J = A$ or B, and $\alpha = 1$ or 2 correspond to first- and second-neighbor interactions, respectively. The A–A potentials $w_{AA,\alpha}$ are irrelevant for the calculation of $\{B|A\}$. Of course, they are crucially important in determining the initial $\{A\}$ and the reaction rate, as will become apparent in the next sections.

Figure 1 shows a 12-site colony on a square lattice. Some of the sites are occupied by the immobile A's, others by the mobile B's, and the rest are vacant. The state (or configuration) of the cluster is fully specified by u and σ, which denote, respectively, the sets of sites occupied by A's and B's. For the example in Fig. 1, $u = (1, 7, 9, 11)$ and $\sigma = (2, 4, 6)$. Also, u and σ uniquely specify $E(\sigma | u)$, the "internal" energy of the cluster due to B–B and A–B interactions *within* the cluster; e.g., for the configuration in Fig. 1a, $E(\sigma | u) = 2w_{BB,2} + 4w_{AB,1}$. Note that $E(\sigma | u)$ does not include A–A interactions. $E(\sigma | u)$ takes into account all first- and second-neighbor interactions associated with B atoms which in configuration σ happen to occupy either one or both of the two central sites (1 and 2 in Fig. 1b) of the cluster. In the next section we shall calculate the rate of reaction (1) by summing (with proper weighting) over the probabilities of all configurations involving an A–B pair in the center of the 12-site colony. This is the main reason for choosing the rectangular shape for the colony. Note, however, that to calculate these probabilities we must consider on the same basis all possible configurations u, σ, including those in which the occupation of the central site is not A–B.

The interaction energy of B atoms located on the (ten)perimeter sites (3,..., 12) of the cluster with neighboring B or A atoms outside the cluster is taken into account in an average fashion, as in mean field theories. We express this interaction energy with the surroundings as $E_s(\sigma) = n_c(\sigma)\psi + n_l(\sigma)\phi$, where ψ and ϕ are two mean field (Lagrange) parameters

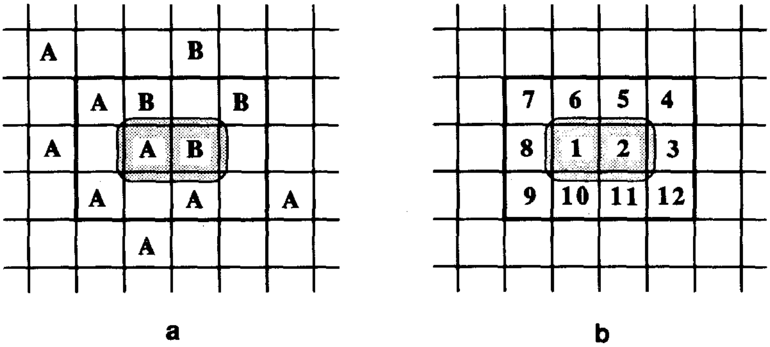

Fig. 1. (a) An example of a 12-site cluster on a square lattice. The configuration of this particular cluster is $u = (1, 7, 9, 11)$, $\sigma = (2, 4, 6)$. (b) The numbering convention of cluster sites.

to be determined later. ψ measures the average interaction energy of a B atom located at one of the four "corner" sites (4, 7, 9, 12) with the surroundings, and ϕ is the corresponding quantity for the six "edge" sites (3, 5, 6, 8, 10, 11). $n_c(\sigma)$ and $n_e(\sigma)$ are the numbers of B atoms occupying corner and edge sites, respectively, in configuration σ. The use of only two energy parameters ψ and ϕ corresponds to the assumption that all corner sites within a given colony (i.e., a given u) as well as those in different colonies are equivalent, and similarly for the edge sites. This of course is true only in an average sense, i.e., after averaging over all 12-site colonies corresponding to a given $\{A\}$, as clarified below. Finally, it should be noted that instead of ψ and ϕ, we could equivalently express $E_s(\sigma)$ as $E_s(\sigma) = n_1(\sigma)\, v_1 + n_2(\sigma)\, v_2$, where v_1 and v_2 are two mean field parameters representing the average nearest and next nearest neighbor interactions between the ten perimeter sites 3–12 and the surroundings. $n_1(\sigma)$ and $n_2(\sigma)$ are the numbers of nearest and next neighbor bonds corresponding to σ, with B atoms located at corner sites contributing 2 to $n_1(\sigma)$ and 3 to $n_2(\sigma)$. The corresponding contributions of the edge atoms are 1 and 2. It is easily verified that the two representations are equivalent, i.e., ψ and ϕ uniquely determine v_1 and v_2 and vice versa.

Let $P(\sigma \mid u)$ denote the (conditional) probability that a 12-site colony with a given A configuration u will be populated by B's as specified by σ. We express this quantity in the grand canonical form

$$P(\sigma \mid u) = \frac{1}{\Xi_u} \exp\{-\beta[n(\sigma)\, \mu_B + E(\sigma \mid u) + E_s(\sigma)]\}$$

$$= \frac{1}{\Xi_u} \lambda_B^{n(\sigma)} \prod_{\alpha = 1,2} \chi_{AB,\alpha}^{n_{AB,\alpha}(\sigma,u)} \chi_{BB,\alpha}^{n_{BB,\alpha}(\sigma,u)} \zeta_\alpha^{n_\alpha(\sigma)} \tag{2}$$

with Ξ_u, the grand partition function (for a given u), defined as usual through the normalization condition for $P(\sigma \mid u)$, i.e.,

$$\sum_\sigma{}' P(\sigma \mid u) = 1 \tag{3}$$

in which the prime on the sum restricts the summation to those σ compatible with u (i.e., no B should occupy a site already taken by A).

In Eq. (2), μ_B is the chemical potential of the adsorbed B atoms, and $\lambda_B = \exp(-\beta\mu_B)$ is the absolute activity ($\beta = 1/kT$). Clearly, μ_B must be the same for all B's anywhere on the lattice. $n(\sigma)$ is the total number of B atoms in the cluster in configuration σ. The second line in (2) follows from an explicit representation of the two energy terms $E(\sigma \mid u)$ and $E_s(\sigma)$ as sums of first ($\alpha = 1$) and second ($\alpha = 2$) neighbor contributions. Namely, $\chi_{IJ,\alpha} = \exp(-\beta w_{IJ,\alpha})$, where, as before, $w_{IJ,\alpha}$ is the interaction potential of order α between I and J. Here $n_{AB,1}(\sigma, u)$ is the number of nearest neighbor AB bonds for a cluster in state σ, u (e.g., for Fig. 1a this number is 4), etc. Finally, $\xi_\alpha = \exp(-\beta v_\alpha)$, where v_1 and v_2 are the mean field parameters measuring the interaction energies between perimeter B atoms and the surroundings, as defined above.

Equation (2) involves three parameters, λ_B, ξ_1, and ξ_2 (or μ_B, v_1, and v_2), which can be determined with the aid of self-consistency (conservation) conditions. To do so, we will have to average $P(\sigma \mid u)$ over all possible u's, i.e., over all possible A-atom configurations of the 12-site colony. We thus define $f_u = N_u/N$ as the fraction of 12-site colonies with A configuration specified by u. Of course, f_u is uniquely determined by $\{A\}$, the overall, fixed distribution of A atoms on the lattice. In the general case $\{A\}$ is an arbitrary distribution, and N_u, the number of u clusters, is determined by direct "scanning" of the lattice. For an infinitely large lattice all choices of sufficiently large random samples of 12-site colonies should give identical results. In our simulations of reaction rates, where the distribution of A's is modeled by MC simulations on lattices whose size M is typically on the order of 100×100 sites (with periodic boundary conditions), we simply count all colonies. Note that since each site can serve four times as site 1 (corresponding to the four rotations of the 12-site rectangle in Fig. 1b), the total number of clusters is $N = 4M$ (partially overlapping clusters are counted as different objects).

The averaging over all possible u yields an "average cluster" in which the average occupation of each of the 12 sites by a B atom must be θ_B. We can thus write 12 equations expressing these conditions. Of course, only three of these equations are different, because the two central sites (1, 2) correspond to the same equations and similarly for the four corner sites (4, 7, 9, 12) and the six edge sites (3, 5, 6, 7, 10, 11) (Actually, sites 3 and 8 could be regarded and treated as different from 5, 6, 10, 11). The equations are

$$\sum_u f_u \sum_\sigma{}' P(\sigma \mid u)\, b_i(\sigma) = \theta_B \tag{4}$$

where $b_i(\sigma)$ is a step function, $b_i(\sigma) = 1$ if in configuration σ site i is occupied by B, and 0 otherwise. Substituting $P(\sigma \mid u)$ from (2) into (4) and solving the equations for, say, $i = 1, 4$, and 5 yields the values of λ_B, ξ_1, and ξ_2 which characterize $P(\sigma \mid u)$. Note that $P(\sigma \mid u)$ contains all the information we have about $\{B \mid A\}$. This of course is not enough for specifying $\{B \mid A\}$, especially when long-range correlations become important (see Section 3), but in many cases $P(\sigma \mid u)$ provides all the information one needs.

2.2. Reaction Rate

The rate of reaction (1) on a surface covered by immobile A atoms organized according to $\{A\}$ can be expressed as a (weighted) sum over all lattice sites m,

$$-\frac{d\theta_A}{dt}=R=\frac{1}{M}\sum_m \delta_m(A)\, q_m \tag{5}$$

Here, $\delta_m(A)=1$ if site m is occupied by an A atom and 0 otherwise. q_m is the reaction probability per unit time for site m. Every A atom has a finite reaction probability, provided a B atom can reach at least one of its four nearest neighbor sites. (We ignore the possibility of reaction between A and B which are not nearest neighbors.) Each lattice site m which is already occupied by an A atom can serve as site 1 of a 12-site cluster, as in Fig. 1. Each of its four nearest neighbors can serve as site 2. Thus, each site m appears as site 1 in four different clusters, all of which contribute to q_m. In addition to the A atom on site 1, each of these clusters may contain other A atoms, on sites 2,..., 12, in a configuration specified by u. All clusters with the same u are assumed to be equally reactive (an assumption which becomes exact if we neglect the effects of A atoms outside the cluster). $q(u)$, the reaction probability of an A atom situated on site 1 of a u cluster is, in turn, a sum of contributions from all possible configurations σ of B atoms on the remaining sites of the cluster; the corresponding contribution to $q(u)$ will be denotd as $q(\sigma, u)$. We model this quantity by the Arrhenius form

$$q(\sigma, u)=b_2(\sigma)\, \nu_R \exp\{-\beta[\varepsilon_0+\Delta\varepsilon_a(\sigma, u)]\} \tag{6}$$

where, as in (4), $b_2(\sigma)=1$ if site 2 is occupied by a B atom and 0 otherwise (B atom on site 2 is a necessary condition for reaction). ν_R is a frequency factor (for surface reactions typically $\sim 10^{13}$–$10^{16}\ \text{sec}^{-1}$), which we assume to be independent of u and σ. Here ε_0 is the activation energy of an isolated AB pair and $\Delta\varepsilon_a(\sigma, u)$ is the excess activation energy due to lateral interactions of the reactive pair on sites 1 and 2 with its ten neighbors on sites 3,..., 12. The simplest model takes $\Delta\varepsilon_a(\sigma, u)$ as a sum of all nearest and next nearest neighbor interaction energies, e.g., for the cluster in Fig. 1a, $\Delta\varepsilon_a(\sigma, u)=3w_{AA,2}+2w_{AB,1}+2w_{BB,2}$.

With the explicit expressions for $q(\sigma, u)$ from (6) and $P(\sigma\,|\,u)$ from (2), the rate of reaction (1), expressed formally in (5), can now be calculated from

$$R=\frac{1}{M}\sum_m \delta_m(A) \sum_{u\in m} q(u)=\frac{1}{M}\sum_m \delta_m(A) \sum_{u\in m} \sum_\sigma P(\sigma\,|\,u)\, q(\sigma, u) \tag{7}$$

where the sum over $u \in m$ refers to the four A-atom configurations u, corresponding to the four 12-site clusters prescribed by the A atom on site m.

2.3. Simulation of Temperature-Programmed Reactions

Temperature-programmed reaction spectroscopy (TPRS) is one of the principal experimental techniques for extracting kinetic data, such as activation energies and reaction orders of surface reactions.(12,13) The basic idea of the method is to coadsorb A and B at temperature T_0 which is too low for reaction to take place. (Note, however, that one reactant, say A, may be adsorbed at high temperature and then the system is quenched to a lower temperature, at which B is added to the surface. Alternatively, both A and B are adsorbed at or below T_0.) From this moment on, the temperature is raised monotonically, e.g., linearly, $T(t) = T_0 + \gamma t$ and R is measured as a function of T. In general, R will first increase following the temperature rise, but eventually will fall off because of the consumption (and removal) of reactants from the system. The result is that $R(T)$ shows one or several peaks (i.e., "spectrum") at intermediate temperatures. Different peaks often imply different types of adsorption sites or different reaction mechanisms. The locations and shapes of the peaks contain information on the activation energies and the molecularities of the processes taking place on the surface. The "inversion" of a TPR spectrum, i.e., the extraction of the kinetic parameters from the spectrum, is not unique. Thus, theoretical simulations of such experiments are instructive for shedding light on some of the ambiguities involved.

Our theoretical model for TPRS experiments consists of a combination of MC simulations and the modified lattice gas model for $\{B|A\}$. For each temperature, starting with T_0, we calculate $P(\sigma|u)$ and $q(\sigma, u)$ for the given $\{A\}$ and θ_B, as described above. These quantities are used to calculate q_m for all A atoms on the surface [cf. (5) and (6)]. The probability that the A atom on site m will react during a short time interval Δt is $q_m \Delta t$. At this point a random sampling (MC) procedure is employed to decide whether the atom on m does or does not react during Δt. All A's which happened to react during Δt are removed from the surface, the rate R and the new $\{A\}$ are recorded, θ_B is adjusted (i.e., one B removed together with each A), and the temperature is raised to $T + \Delta T$. Now the entire process repeats itself for the new temperature, and so on until the reaction terminates.(7)

3. RESULTS AND DISCUSSION

In this section we present some results of a few representative simulations of temperature-programmed reactions. We do not intend to reproduce or predict the behavior of a specific experimental system, but rather to examine the accuracy of the lattice gas approximation formulated in the previous section. (Comparison with experimental studies will be reported elsewhere.(17)) To this end, we compare two schemes for calculating the time evolution of the reactive bimolecular system. The first procedure is our combined MC–lattice gas (hereafter the BPA/MC or, simply, the BP) scheme outlined in Section 2.3. The second is a full MC simulation for all the kinetic processes, which we use as a reference for comparison. In fact, the difference between the two procedures pertains only to the calculation of $\{B|A\}$. In the first scheme, $\{B|A\}$ is calculated using the BPA, while in the full MC simulation the motion and distribution of B on the surface is modeled by (conserved) MC dynamics. The removal of A's due to reaction is modeled equally in both schemes.

Various quantities have been analyzed and contrasted in order to compare the two modeling procedures. Thes include reaction rates (i.e., TPR spectra), total and local populations, sizes and shapes of A islands, and a variety of averages.(17) Here we skip a systematic and detailed comparison and concentrate on demonstrating and discussing "snapshots" of the adspecies lateral distributions as predicted by the two schemes. All the results shown below correspond to the same set of molecular parameters. The lateral interaction energies, in kcal/mole, are $w_{AA,1} = \infty$, $w_{AA,2} = 1.6$, $w_{BB,1} = 4.0$, and $w_{AB,1} = w_{AB,2} = 3.0$; all other $w_{IJ,\alpha}$ are identically zero. We have used $\nu_R = 10^{15}\ \text{sec}^{-1}$ and $\varepsilon_0 = 28$ kcal/mole [cf. (6)]. In the simulation of temperature-programmed reactions the temperature was raised linearly, $T = T_0 + \gamma t$, with $T_0 = 300$ K and $\gamma = 10$ K/sec. All simulations, both in the full MC and the BP schemes, have been carried out on a square lattice of 100×100 sites with periodic boundary conditions.

A few remarks should be made about the preparation of the initial distribution $\{A, B\}$ characterizing the system at the onset of the temperature sweep. Motivated by experimental results for the O + CO reaction(13) on Pd(100) (square 2D lattice), in which O corresponds to our A and CO to our B, the following conditions were assumed: At $t = 0$, A atoms are randomly adsorbed on the surface and the system is allowed to evolve until B is adsorbed at $t = t_1$. In the cases considered below, t_1 was chosen long enough for A (10,000 MC steps) to organize in long-lived islands.(2,7) During this stage we have used $w_{AA,1} = \infty$ and $w_{AA,2} = 1.6$ kcal/mole as already mentioned, but in addition, attractive third-neighbor potentials $w_{AA,3} = -0.6$ kcal/mole were also included in order to favor the $p(2 \times 2)$

structure as the thermodynamically preferred state.(13) Note, however, that the $p(2\times 2)$ adlayer saturates at $\theta_A = 0.25$. Hence, if θ_A or $\theta_A + \theta_B$ exceeds this value, a transition to the less stable $c(2\times 2)$ structure should be expected, at least in certain regions of the lattice. This indeed happens after B is added at t_1. In the simulations we let A and B evolve together to a new state for another period of time t_2. In all the results shown below, t_2 ($=10{,}000$ MC steps) is long enough so that $\{A, B\}$ changes extremely slowly after $t_1 + t_2$. Because of the strong B–B and B–A repulsions, the addition of B's induces, at high enough coverages, compression of the $p(2\times 2)$ domains of A into $c(2\times 2)$ islands, as observed experimentally.(13) During the first two steps (i.e., when $t \leqslant t_1 + t_2$) the temperature is kept below the reaction threshold.

At $t = t_1 + t_2$ we set $t = 0$ again and start the reactive stage by increasing T. At this moment we also start the comparison between the two modeling schemes. (At this stage we set $w_{AA,3} = 0$; we ignore nonreactive desorption of A or B). In the full MC model we simply continue to simulate the motion of B and the $A + B$ reaction by MC sampling. On the other hand, in the BP scheme, all we need are the *probabilities* of finding B atoms on A-free sites. These are dictated by $\{A\}$ and therefore in showing snapshots of the lattice in the BP model we cannot and need not specify where exactly the B atoms are located. Figures 2–4 show such snapshots of (40×40 sections of) the lattice corresponding to three different initial coverages of A and B.

Figure 2 compares the MC and BP modes for relatively low initial coverages, $\theta_A^0 = 15$ and $\theta_B^0 = 0.10$. The initial $\{A\}$ at $t = 0$ and $T_0 = 300$ K is the same in both models. The next snapshot is taken at 440 K (i.e., 4 secs later, when R reaches its maximum value). The pattern of $\{A\}$ is very similar in both models. More importantly, θ_A and θ_B have changed by exactly the same amount, indicating that R is identical. Similar agreement is indicated by the last snapshots, which are taken when the reaction is nearly over. Thus, Fig. 2, and other results not discussed here, reveal that the BP approximation for $\{B|A\}$ is excellent for the relatively low coverages in Fig. 2. This is not surprising because, after all, the BPA takes into account exactly all relevant correlations within the fairly large 12-site cluster. For the coverages considered in Fig. 2, long-range correlations between the B atoms are weak and are not expected to affect R.

Considerably higher coverages, $\theta_A^0 = \theta_B^0 = 0.2$, correspond to the initial state in Fig. 3. The snapshots taken at 400 and 440 K reveal some differences between the $\{A\}$ patterns, but the coverages at intermediate ($T = 400$ K) and late ($T = 440$ K) stages are essentially identical, and so are the rates, for both models. The comparison of the rates is, of course, more informative than the $\{A\}$ patterns, whose time evolution is governed by

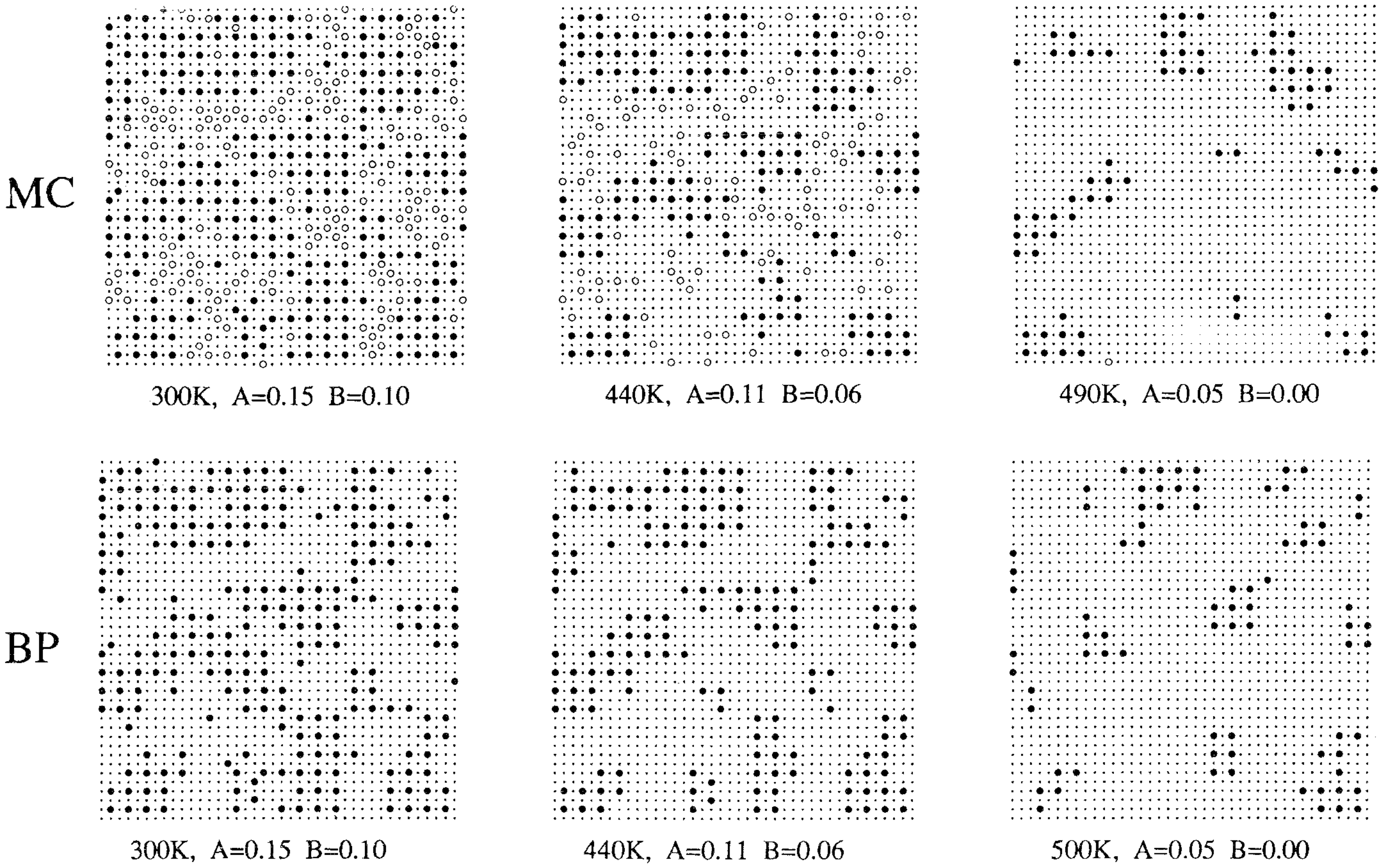

Fig. 2. Snapshots from simulations of a temperature-programmed reaction for relatively low initial coverages ($\theta_A^0 = 0.15$, $\theta_B^0 = 0.10$). The upper three frames (marked MC) are obtained from a full MC simulation. The solid circles represent the immobile *A* atoms, the open ones correspond to the rapidly diffusing *B*'s. The dots mark the lattice sites. The lower three frames (marked BP) display the time evolution of the distribution of *A* atoms (solid circles) in the course of reaction with *B* when the distribution of *B* atoms is calculated by the modified BP approximation. The *B* atoms are not shown here, as explained in the text. The numbers under each frame mark the temperature, the coverage of *A*, and the coverage of *B*. Note that at these low coverages the *A* atoms are initially organized in the energetically most favorable $p(2\times 2)$ structure.

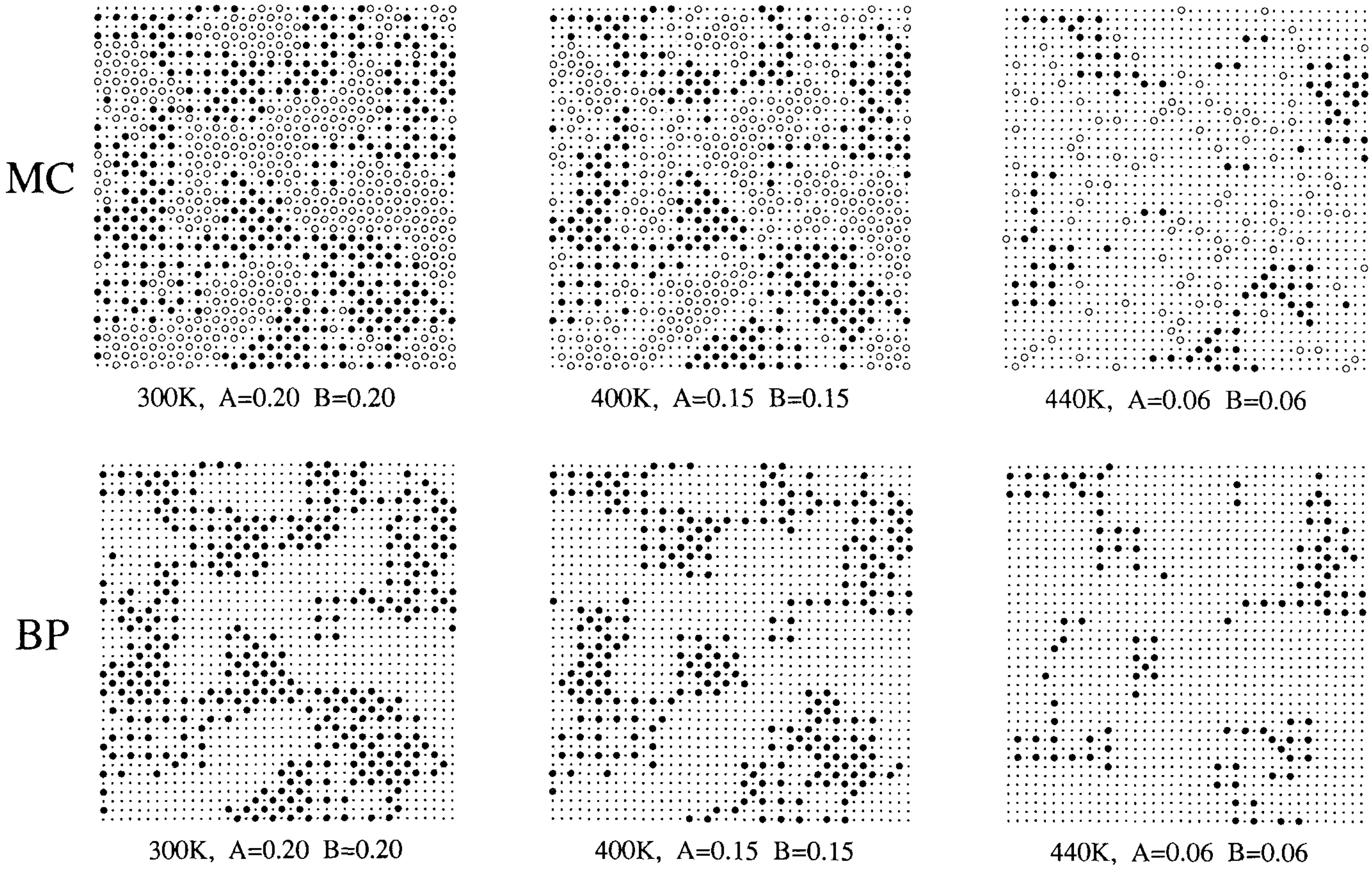

Fig. 3. The same as in Fig. 2 but with higher initial coverages ($\theta_A^0 = 0.20$, $\theta_B^0 = 0.20$). Strong *B–B* and *A–B* repulsions compress (most of) the *A* atoms from the $p(2\times2)$ to the $c(2\times2)$ islands. Note that the populations of *A* and *B* in the two schemes are equal at equal temperatures (times), indicating identical reaction rates.

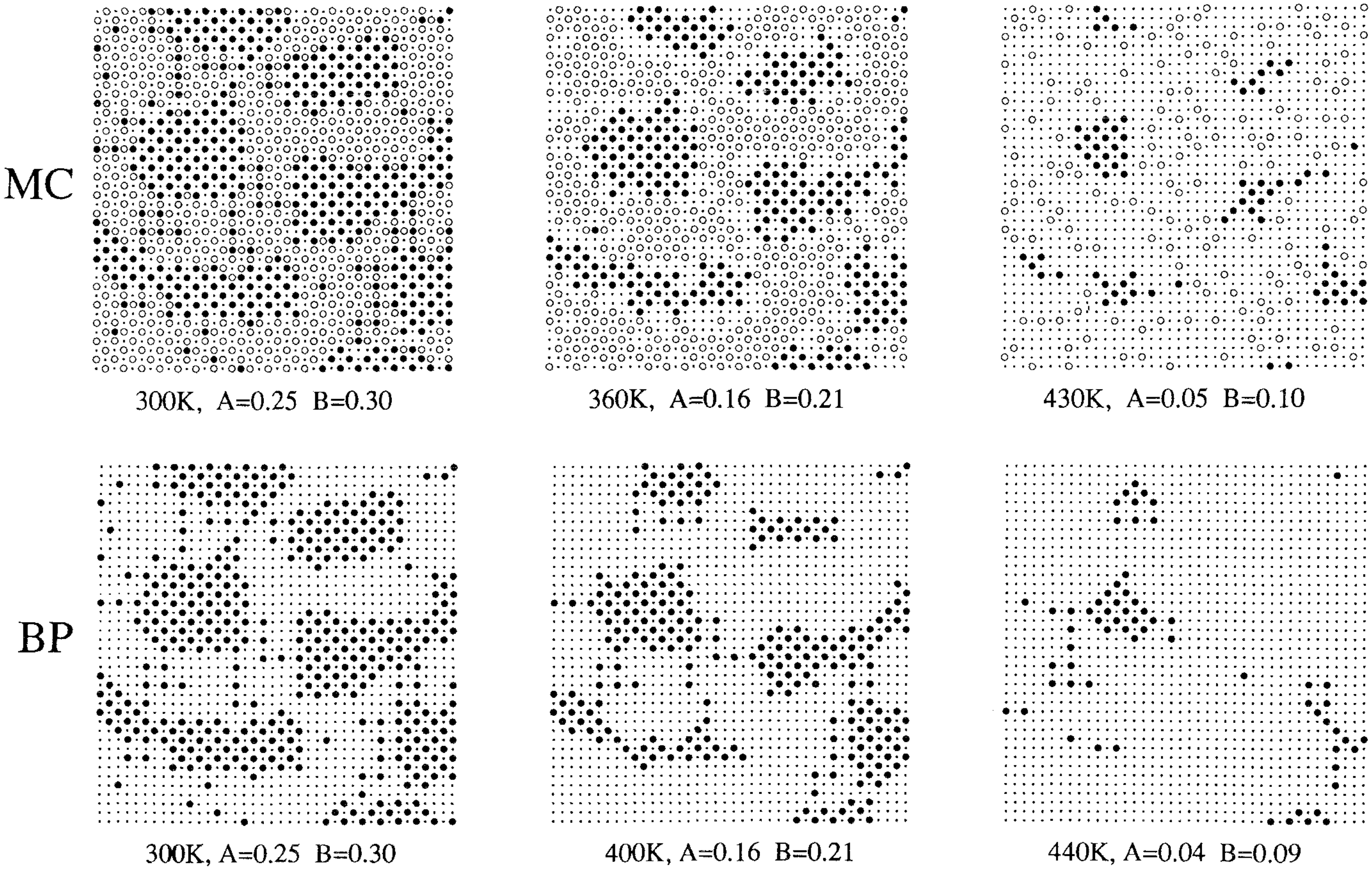

Fig. 4. The same as in Fig. 2 but with very high initial coverage ($\theta_A^0 = 0.25$, $\theta_B^0 = 0.30$). Here, initially all *A* atoms are organized in $c(2\times2)$ domains. Because of the high coverage and despite *A–B* repulsions, some of the *B* atoms penetrate into *A* islands. These are highly energetic and react first, as revealed by the pictures describing the full MC calculation. As explained in the text, the BP procedure is less satisfactory at these high coverages because it cannot account for the very long range correlations between the *B* atoms.

probabilistic rules. In other words, differences between the two $\{A\}$'s are partly simple statistical fluctuations. Thus, the BPA gives good results even when the surface is in fact fully covered by A and B.

Finally, a case of very high initial coverage is shown in Fig. 4. The first picture in the MC model reveals very clearly that the positions of B atoms in one region of the lattice are strongly correlated [via the $c(2\times 2)$ structure formed by B's] with those B's in distant regions. In fact, at these very high coverages, some B atoms are pushed into the interior of A islands, resulting in "high energy," and thus highly reactive A–B pairs. Inspection of the second snapshot of the MC scheme indicates that these indeed have been the first atoms to react. Unlike in the full MC scheme, the BPA, which takes only local correlations into account, will always favor lower energy configurations. Thus, for example, this model gives negligible probability for penetration of B's into A islands. Correspondingly, the rate predicted by the BP/MC scheme will be lower, as indeed is indicated by the data in Fig. 4. Similarly, the TPR spectra calculated by the two schemes are quite different, especially at the early stages of the temperature ramp.

4. CONCLUDING REMARKS

In the previous sections we have tried to show that a seemingly simple process, such as a bimolecular reaction on a two-dimensional lattice, can in fact be very intricate and present various theoretical challenges involving both kinetic and thermodynamic issues. Monte Carlo and other computer simulation techniques are rapidly developing into an almost standard (and gradually less expansive) tool for systematic analyses of equilibrium and nonequilibrium systems.(18) Nevertheless, in many cases, alternative, "more conservative" approximate but analytical models can be used to replace (or supplement) substantial parts of a comprehensive computer simulation, thereby not only reducing the computational effort but also introducing new physical insights. Our problem is, in fact, just one example demonstrating that in a complex nonequilibrium system involving kinetic processes which take place on very different time scales, some degrees of freedom are always in a state of "local equilibrium." These modes can of course be treated by standard or appropriately modified equilibrium methods. In our specific problem the rapidly equilibrating "degree of freedom" has been the 2D translation of the mobile atoms whose motion is hindered and distorted by the presence of the immobile atoms on various lattice sites. To account for these effects, we have presented here a (nontrivial) variation of a familiar lattice gas approximation and demonstrated its combination with a MC procedure in the framework of a comprehensive kinetic modeling scheme. We believe that combinations of this sort may be instructive in various other complex physicochemical systems.

ACKNOWLEDGMENT

This research was supported by the Fund for Basic Research administered by the Israel Academy of Sciences, and by V.D.I. Düsseldorf, Germany, via the National Council for Research and Development, Israel. The Fritz Haber Research Center is supported by the Minerva Gesellschaft für die Forschung, mbH, Munich, Federal Republic of Germany.

REFERENCES

1. T. Engel and G. Ertl, *Adv. Catal.* **28**:1 (1979); T. Ertl in *Catalysis*, J. R. Anderson and M. Boudart, eds. (Springer, Berlin, 1983), Vol. 4, p. 210.
2. M. Silverberg and A. Ben-Shaul, *J. Chem. Phys.* **87**:3178 (1987); *Chem. Phys. Lett.* **134**:491 (1987).
3. T. L. Hill, *Statistical Mechanics* (McGraw-Hill, New York, 1956), T. L. Hill, *Introduction to Statistical Thermodynamics* (Addison-Weseley, Reading, Massachusetts, 1960).
4. K. Huang, *Statistical Mechanics* (Wiley, New York, 1963).
5. D. L. Adams, *Surf. Sci.* **42**:12 (1974); see also H. Asada, *Surf. Sci.* **159**:393 (1985).
6. T. L. Einstein, *Crit. Rev. Solid State Mater. Sci.* **7**:261 (1978); J.-P. Muscat, *Phys. Rev. B* **30**:8136 (1986).
7. M. Silverberg, A. Ben-Shaul, and F. Rebentrost, *J. Chem. Phys.* **83**:6501 (1985).
8. G. S. Grest and D. J. Srolovitz, *Phys. Rev. B* **30**:5150 (1984); P. S. Sahni, G. Dee, J. D. Gunton, M. Phani, J. L. Lebowitz, and M. Kalos, *Phys. Rev. B* **24**:410 (1981).
9. J. D. Gunton, M. San Miguel, and P. S. Sahni, in *Phase Transitions*, C. Domb and J. L. Lebowitz, eds. (Academic Press, London, 1983), Vol. 8, Chapter 3.
10. M. G. Lagally, G.-C. Wang, and T. M. Lu, *Crit. Rev. Solid State Sci. Mater. Sci.* **7**:233 (1978); E. D. Williams, W. H. Weinberg, and E. C. Sobrero, *J. Chem. Phys.* **76**:1150 (1982); M. Trigides, P. K. Wu, W. Moritz, and M. Lagally, *Ber. Bunsenges. Phys. Chem.* **90**:277 (1986).
11. B. Poelsema, L. K. Verheij, and G. Comsa, *Phys. Rev. Lett.* **51**:2410 (1983); see also D. K. Dacol, H. Rabitz, and R. B. Gerber, *J. Chem. Phys.* **86**:1616 (1987).
12. J. L. Gland and E. B. Kollin, *J. Chem. Phys.* **78**:963 (1983).
13. E. M. Stuve, R. J. Madix, and C. Brundle, *Surf. Sci.* **146**:155 (1984).
14. H. Reiss, *Adv. Colloid Interface Sci.* **7**:1 (1977).
15. H. Reiss, in *Advances in Chemical Reaction Dynamics*, P. M. Rentzepis and C. Capellos, eds. (D. Reidel, 1986), p. 71.
16. H. Reiss, *J. Stat. Phys.* **6**:39 (1972).
17. M. Silverberg and A. Ben-Shaul, to be published.
18. K. Binder, ed., *Monte Carlo Methods in Statistical Physics*, 2nd ed. (Springer, Berlin, 1986); *Applications of the Monte Carlo Method in Statistical Physics*, 2nd ed. (Springer, Berlin, 1987).